



## ■ BIOMECHANICS

# Effect of surface matching mismatch of focal knee articular prosthetic on tibiofemoral contact stress using finite element analysis

J-A. Lee,  
Y-G. Koh,  
P. S. Kim,  
J-H. Park,  
K-T. Kang

From Yonsei University,  
Seoul, South Korea

## Aims

Focal knee arthroplasty is an attractive alternative to knee arthroplasty for young patients because it allows preservation of a large amount of bone for potential revisions. However, the mechanical behaviour of cartilage has not yet been investigated because it is challenging to evaluate in vivo contact areas, pressure, and deformations from metal implants. Therefore, this study aimed to determine the contact pressure in the tibiofemoral joint with a focal knee arthroplasty using a finite element model.

## Methods

The mechanical behaviour of the cartilage surrounding a metal implant was evaluated using finite element analysis. We modelled focal knee arthroplasty with placement flush, 0.5 mm deep, or protruding 0.5 mm with regard to the level of the surrounding cartilage. We compared contact stress and pressure for bone, implant, and cartilage under static loading conditions.

## Results

Contact stress on medial and lateral femoral and tibial cartilages increased and decreased, respectively, the most and the least in the protruding model compared to the intact model. The deep model exhibited the closest tibiofemoral contact stress to the intact model. In addition, the deep model demonstrated load sharing between the bone and the implant, while the protruding and flush model showed stress shielding. The data revealed that resurfacing with a focal knee arthroplasty does not cause increased contact pressure with deep implantation. However, protruding implantation leads to increased contact pressure, decreased bone stress, and biomechanical disadvantage in an in vivo application.

## Conclusion

These results show that it is preferable to leave an edge slightly deep rather than flush and protruding.

**Cite this article:** *Bone Joint Res* 2023;12(8):497–503.

**Keywords:** Finite element analysis, Focal knee implant, Cartilage

## Article focus

■ The effect of depth level of focal articular prosthetic on tibiofemoral contact stress using finite element analysis.

■ The inserted level is important for the lifespan of focal knee arthroplasty and successful surgery.

## Key messages

■ The biomechanical effects depend on the inserted level of focal knee arthroplasty.

## Strengths and limitations

■ This study showed that the inserted level of focal knee arthroplasty has a significant effect on the opposite surfaces based on

Correspondence should be sent to  
Kyoung-Tak Kang; email:  
tagi1024@gmail.com

doi: 10.1302/2046-3758.128.BJR-  
2023-0010.R1

*Bone Joint Res* 2023;12(8):497–  
503.

the contact pressure evaluated through the computational simulation of the deep model.

- This study did not compare the actual clinical data for contact stress and pressure.

## Introduction

Full-thickness cartilage defects can cause early osteoarthritis (OA).<sup>1,2</sup> If conservative treatment is not successful, other surgical approaches are possible. A localized treatment that maintains the surrounding and opposite healthy cartilage is preferred.<sup>3</sup> The current surgical options for treatment of localized cartilage defects are primarily aimed at biological repair, including joint lavage and debridement, subchondral drilling, osteochondral transplantation, and autologous chondrocyte transplantation.<sup>3</sup> Metallic inlay resurfacing was developed to accurately match the metal implant surface to the patient's articular cartilage surface to fill the defect and restore a smooth and continuous articulating surface.<sup>4</sup> In addition, osteochondral transplantation is an effective treatment for such defects, but the outcome is dependent on the stability and restoration of surface congruency in other parameters.<sup>5</sup> The rationale of the device is to provide an additional treatment layer for management of focal defects after biological measurements have been exhausted or are deemed unsuitable for middle-aged or elderly patients. Healthy cartilage, bone, and soft-tissue are restored until conventional joint arthroplasty becomes necessary.<sup>6</sup>

An implant fabricated from a hard material imposes specific requirements on the surgeon's instruments and on the implant itself. The surgery has to be performed with precision so that no part of the implant protrudes above the surrounding cartilage, thereby acting as a plough on the opposing articulating surface. In an attempt to address the requirements for precision, an implant has been developed with a design based on the patient-specific knee curvature from MRI or CT images.<sup>7</sup> The MRI images are used to examine the lesion and provide details to the surgeon, and the implants and guide instruments are manufactured through computer-aided design and manufacturing (CAD/CAM).<sup>7</sup> The success of this approach is dependent on various factors. Since localized implants articulate on healthy unaffected cartilage, it is anticipated that the position of the implant in relation to the adjacent tissues affects the articulating surfaces. It is not yet clear whether it is better, in terms of articulating surface integrity, to place an implant flush with the surrounding cartilage or slightly depressed. Koh et al<sup>5</sup> studied the effect of a mismatch of graft height on contact pressures in the adult swine knee. They demonstrated that normal contact pressures and patterns can be duplicated with flush articular surface grafts.<sup>5</sup> Custers et al<sup>3</sup> evaluated the effect on opposing cartilage quality and osseointegration at various insertion depths. They determined that placement flush to the surrounding cartilage is essential.<sup>3</sup> In addition, they found that positioning the implant flush induced less tibial cartilage degradation

compared to other models. However, their study could not determine a load transmission mechanism to explain how focal knee arthroplasty affects contact pressure on the medial and lateral tibial cartilage.

Therefore, the purpose of this study was to investigate the biomechanical effect of placement depth of focal knee arthroplasty with placement flush, 0.5 mm deep, or protruding 0.5 mm with regard to the level of the surrounding tissue. We investigated contact pressure on articular cartilage and stress on the bone in the tibiofemoral joint regarding focal knee arthroplasty positions.

## Methods

**Development of the focal knee arthroplasty model.** An anatomically precise finite element (FE) model of the lower limb was developed using imaging data obtained from a healthy, skeletally mature young male athlete without knee injury history.<sup>8-10</sup> The model included bony structures of the lower limb with the soft-tissue details of the patellofemoral and tibiofemoral aspects of the knee joint. This computational knee model was developed and validated in Kang et al.<sup>8-10</sup> The bones of our computational knee model were created based on CT data, while the soft-tissues were based on MRI data. The maximum contact stress at the menisci value was compared for validation. The femur and tibia were divided into cortical and cancellous bone. The geometry was simplified using thickness constants of 1 mm for the cortical bone of the femur and tibia.<sup>11,12</sup> The constitutive laws for the cortical and cancellous bone were assumed to be linearly elastic and homogeneous. The cortical bone was considered transversely isotropic, and the following material properties were used:  $E_1 = E_2 = 11.5$  GPa,  $0E_3 = 17$  GPa,  $\nu_{12} = 0.58$ , and  $\nu_{23} = \nu_{13} = 0.31$ .<sup>13</sup> The cancellous bone was considered linear elastic isotropic. The following material properties were used:  $E = 2.13$  GPa and  $\nu = 0.3$ .<sup>13</sup> The articular cartilage was defined as an isotropic and linear elastic material with  $E = 15$  MPa and  $\nu = 0.47$ , where a time-independent and simple compressive load was applied to the knee joint.<sup>14,15</sup> The interfaces between the cartilage and bones were modelled as fully bonded. The menisci were modelled as transversely isotropic linear elastic materials with different mechanical properties in the circumferential, axial, and radial directions.<sup>14,15</sup> The following material properties were used:  $E = 120$  MPa in the circumferential direction,  $E = 20$  MPa in the axial and radial directions,  $\nu = 0.2$  in both the circumferential and radial directions, and  $\nu = 0.3$  in the axial direction.<sup>14,15</sup> To simulate meniscal attachments, each meniscal horn was fixed to the bone using linear spring elements ("SPRINGA" element type) with a total stiffness of 2,000 N/mm at each horn.<sup>11</sup> The cartilage layers were meshed using pentahedral or hexahedral elements, and the menisci were meshed with hexahedral elements. The ligament models were defined as hyperelastic rubber-like materials that showed nonlinear stress strain relationships.<sup>11</sup> The initial ligament strain model was developed based on a previous study.<sup>16</sup> Contact between the femoral cartilage,

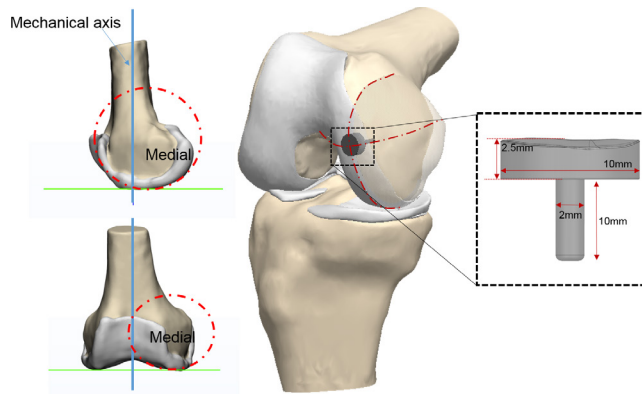


Fig. 1

Parameters and location in the implant geometry.

meniscus, and tibial cartilage was modelled on both the medial and lateral sides.<sup>17,18</sup> The contact option adopted a finite sliding frictionless hard contact algorithm without any penetration in all articulations. We modelled focal knee arthroplasty while maintaining the femoral cartilage curvature. We created the curvature of the femur on the coronal and sagittal planes based on the mechanical axis of the knee for implant location. The implant was inserted at the centre to meet the curvature of the sagittal and coronal planes (Figure 1). The implants had a specific default diameter and size along with a cap height of 2.5 mm. The pin was 2 mm in diameter and 10 mm in length (Figure 1). The radius of curvature of the spherical profile was 10 mm (Figure 1). In addition, the depth of focal knee arthroplasty was modelled with placement flush, 0.5 mm deep and protruding 0.5 mm with respect to the level of the surrounding tissue (Figure 2). Co–Cr material was used for the implant, and its Young's modulus and Poisson's ratio were set as  $E = 220,000$  MPa and  $\nu = 0.3$ , respectively.

We performed a Mesh convergence test to complete the simulation. Convergence was reached if the relative change between the two adjacent meshes was  $< 5\%$ . Mean element sizes were 0.8 mm for cartilage and menisci.

**Loading and boundary conditions.** We applied the same conditions for intact model validation and clinically relevant loading scenarios for the focal knee arthroplasty models. These methods have previously been reported in Koh et al.<sup>19</sup> The bottom of the tibial bone was constrained in all translational and rotational degrees of freedom, while the femur was only restricted in knee flexion, which was fixed at  $0^\circ$  to simulate the short-term gait load of a human knee joint in full extension. A reference point, located in the central region between the lateral and medial femoral epicondyles, was coupled to the femoral surface using the constraint method (Figure 3). An axial compressive load of 1,150 N was exerted on the femoral condyle reference point, which is associated in the gait cycle load in full extension ( $0^\circ$  flexion angle). The model was analyzed using ABAQUS software (version 6.11; Simulia, USA).

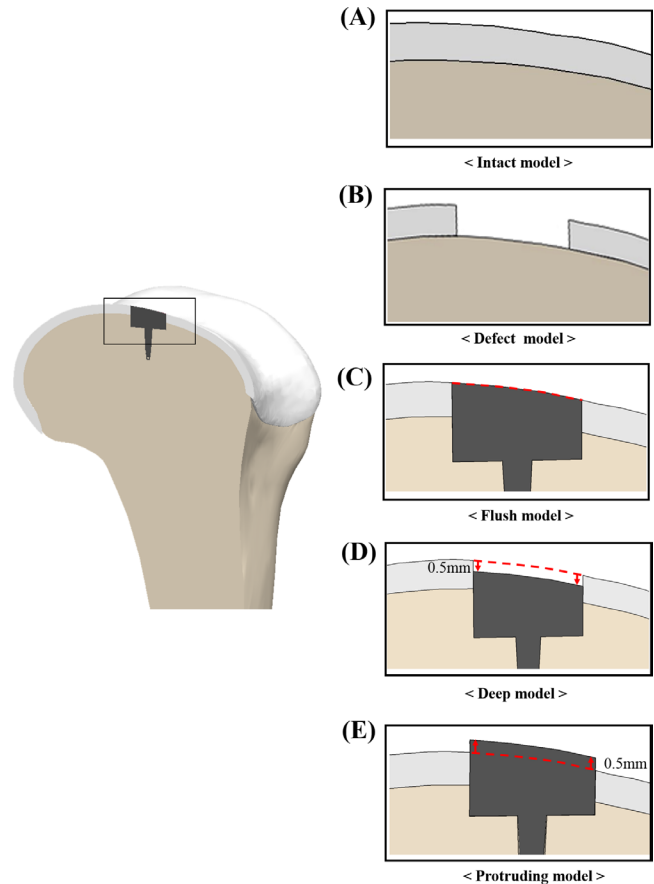


Fig. 2

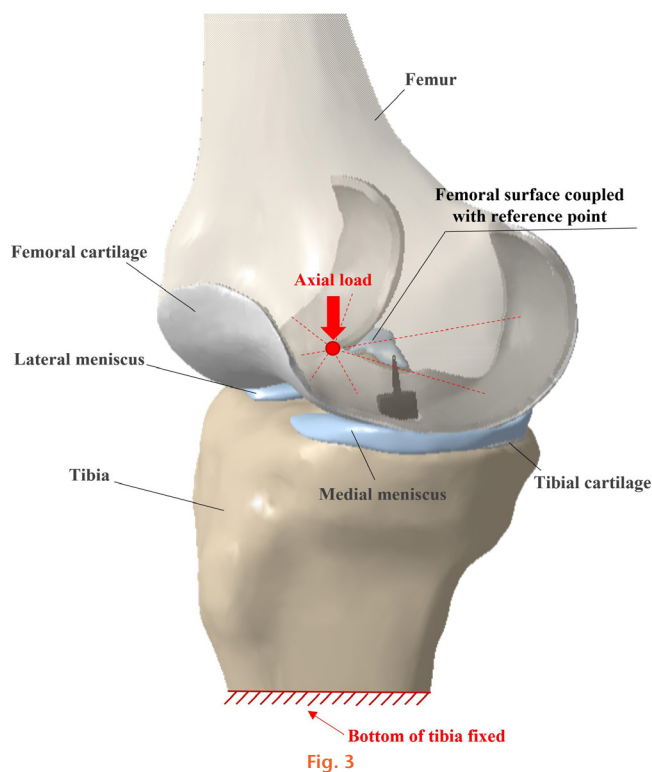
Models of implants under three different insertion positions: a) intact model; b) defect model; c) flush model; d) 0.5 mm deep position compared to surrounding cartilage; and e) 0.5 mm protruding deep position compared to surrounding cartilage.

Contact stresses on the femoral cartilage, as well as the medial and lateral tibial cartilages and stresses on the bone, were evaluated in relation to the implant position.

## Results

For model validation, maximum contact stress on menisci was compared with previous FE results.<sup>16</sup> Maximum contact stresses in the medial and lateral menisci were 3.1 MPa and 1.53 MPa, respectively, under an axial load of 1,150 N, within 4% of maximum contact stresses corresponding to 2.9 MPa and 1.45 MPa from Peña et al.<sup>16</sup> These minor differences can be attributed to variations in geometry, such as differences in the thickness of the cartilage and meniscus in different studies. However, the general consistency between the validation results and those reported in the literature demonstrates the ability of the FE model to produce reasonable results.

Figure 4 shows maximum contact stress on the femoral cartilage and implant for intact, defect, and focal knee models for various implant position depths. On the medial femoral cartilage (implant), the deep, flush, and protruding models demonstrated that maximum contact stress increased by 11%, 104%, and 288%, respectively,



Schematic for boundary and loading conditions.

compared to the intact model. On the lateral femoral cartilage, the focal defect model showed that maximum contact stress increased by 14% in comparison with the intact model. The contact stress of the flush, protruding, and deep models decreased compared to that of the intact model.

Figure 5 shows the contact pressure on the lateral and medial tibial cartilages for the intact, defect, and focal knee models with various implant position depths. On the medial tibial cartilage, maximum contact stress in the focal defect model increased by 9% compared to the intact model. The protruding model exhibited a 104% increase, while the flush model increased by 41% compared to the intact model in maximum contact pressure. On the lateral tibial cartilage, maximum contact stress of the focal defect model increased by 10% compared to the intact model. On the contrary, the flush and protruding models decreased by 17% and 61%, respectively, compared to the intact model. However, maximum contact stress on medial and lateral tibial cartilages in the deep model was similar to those in the intact model.

Figure 6 shows the mean von Mises stress on the bone for focal knee models with various implant position depths. The stress on the bone was greatest in the deep model, followed by the flush and protruding models.

## Discussion

The most important finding of this study was that contact pressure on the opposite cartilage in the deep model was similar to that in the intact model. However, contact

pressure on the lateral femoral cartilage in the protruding model was lower than that in the intact model, while contact pressure on the opposite cartilage was more than twice that in the intact model. This finding indicates the risk of progressive degeneration of the tibial cartilage.

The relationship between focal articular injury and OA has not yet been established. The similar biological, mechanical, and macroscopic features show that both conditions exist along a continuum of joint degeneration.<sup>6</sup> The goal of articular cartilage repair procedures is to reduce morbidity and preserve the normal biological and biomechanical properties of intact articular cartilage for restoration of normal joint function. It is a serious challenge for orthopaedic surgeons to treat patients over 40 years of age with full-thickness chondral or osteochondral defects. Considered too old for biological repair of such defects, these patients are primarily treated with conservative, non-surgical approaches, including weight reduction, physical therapy to increase and support musculature, and unloading braces. However, conservative treatment at best ameliorates the symptoms; biomechanical studies have shown that untreated osteochondral defects may lead to increased contact pressures.<sup>20,21</sup>

Guettler et al<sup>22</sup> stated that osteochondral lesions created in the medial femoral condyle appeared to show a statistically significant increase in peak rim stress value compared to knees under normal conditions. In terms of biomechanics, Brown et al<sup>23</sup> demonstrated stress aberrations following imprecise reduction of intra-articular knee fracture. Huber-Betzer et al<sup>24</sup> showed that high-contact pressures are caused adjacent to defects of the knee. This may well interfere with the ability of chondrocytes near these defects to function normally, given the importance of pressure-driven, interstitial fluid flow in normal cartilage.

In one study, animal models indicated that untreated osteochondral defects undergo progressive degenerative changes.<sup>25</sup> Although smaller defects exhibited the capacity for healing,<sup>25</sup> larger defects caused resorption of their osseous walls, formation of large cavitary lesions, collapse of the surrounding articular cartilage and subchondral bone, and degeneration of the opposing tibial articular surface.<sup>25</sup> Defect repairs are crucial to prevent or delay progressive degenerative joint destruction. However, unicompartamental or total knee arthroplasty is a procedure of last resort for some patients. A focal knee resurfacing prosthesis provides an interim or alternative treatment strategy for middle-aged patients with full-thickness cartilage defects. Clinically, Stålmán et al<sup>26</sup> demonstrated the safety of focal knee resurfacing implants and function. As the pain considerably improved, patient satisfaction increased. However, the effects of a metallic implant articulating with the intact opposing tibial articular cartilage remain debatable. There are three fundamental challenges that must be satisfied. First, the implant must be bonded to the living tissue and become securely fixed. Second, the tribological situation

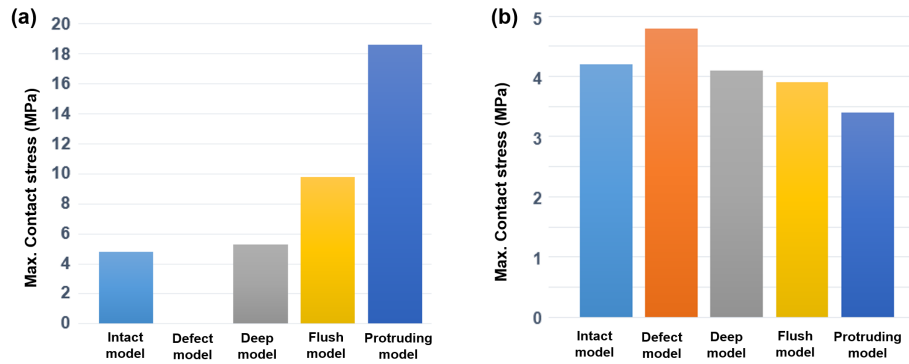


Fig. 4

Comparison of maximum contact stress on a) medial and b) lateral femoral cartilage under different insertion positions.

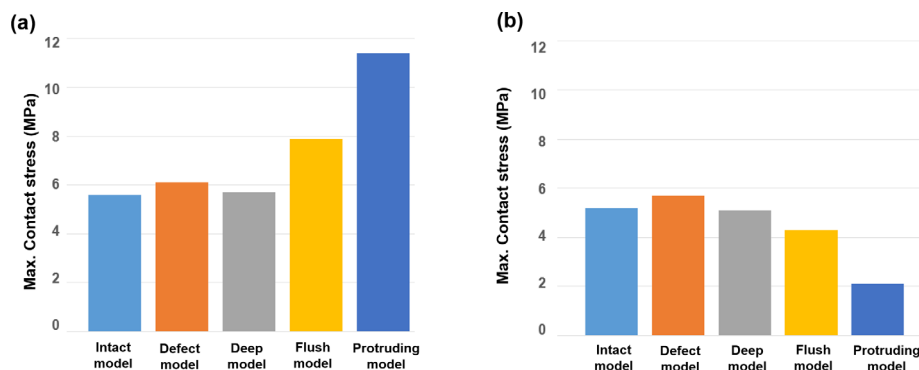


Fig. 5

Comparison of maximum contact pressure on a) medial and b) lateral tibial cartilage under different insertion positions.

must be accepted by the opposing cartilage. Third, the surrounding cartilage must accept the implant.

This computational study evaluated the effect of a surface-matched metallic articular resurfacing device on tibiofemoral contact pressure. We discovered that contact pressure on the lateral femoral cartilage increased in the focal defect model compared to the intact model. Such a trend was also reported by Koh et al.<sup>5</sup> However, the protruding model showed decreased contact stress on the lateral femoral cartilage compared to the intact model, and exhibited the greatest contact stress on the implant (medial femoral cartilage). This is due to a change in load transmission in the knee joints that stems from the loss of mechanical function of the joint line. In addition, more cartilage damage was predicted for the medial tibial cartilage compared to the lateral tibial cartilage, irrespective of the implant position in all models. Such a trend was also found in Custers<sup>3</sup> et al in their rabbit experiment. Less medial and lateral tibial cartilage damage occurred when implants were placed flush or deep as opposed to protruding. The damage of the medial tibial cartilage was most likely caused by implant articulation directly against the tibial cartilage. Interestingly, the lateral tibial cartilage, which did not articulate directly against any implant, was damaged significantly

less than the medial tibial cartilage.<sup>3</sup> Moreover, at this location, damage was significantly associated with the implant and bearing material positioned in the medial compartment. This gradual decrease in cartilage quality has been identified, and might be explained by joint homeostasis as described in a previous report.<sup>27</sup> Therefore, there are a number of factors regarding the physiological equilibrium mechanism of the synovial knee joint. This equilibrium is maintained by the cartilage, subchondral bone, synovial fluid, intact menisci, and ligaments.<sup>3</sup> Implant positioning seems to be an important parameter for the extent of the final cartilage damage. A previous study using medial femoral condyle implants showed that cartilage damage of the tibial plateau was proportional to any elevation of the prosthesis on the adjacent cartilage surfaces, which is in line with our results regarding protruding implants.<sup>28</sup>

An interesting finding was obtained for the protruding model. It showed a 104% increase in contact pressure on the medial tibial cartilage and a 61% decrease in contact pressure on the lateral tibial cartilage compared to the intact model. This might be attributed to the change in load transfer caused by the change of the joint line. Custers et al<sup>3</sup> found that positioning the implant flush led to less tibial cartilage damage, compared to placing it

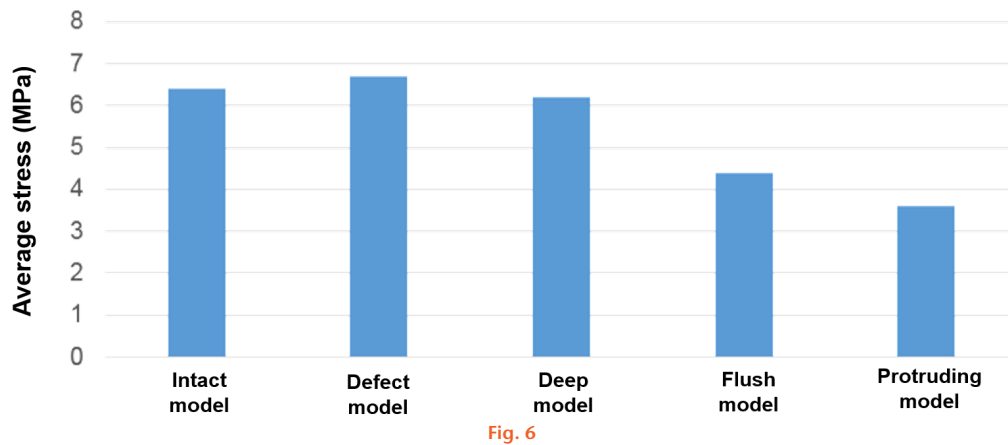


Fig. 6

Comparison of the average stress on the bone for focal knee models under different insertion positions.

1 mm below the surrounding cartilage surface. However, we found that the deep model showed less contact pressure compared to the flush model, and our findings indicated that the deep model may lead to less tibial cartilage damage than the flush model. In addition, our results exhibited good matching with those of Martinez-Carranza et al,<sup>29</sup> who suggested that implants should be recessed approximately 0.5 mm below the surrounding cartilage in their model.

Bone union is important for the success of any metal implant. Theoretically, the deep and flush models showed higher bone contact areas than the protruding model due to implant position. In addition, our results showed greater stress on bone in the deep and flush models compared to in the protruding model. This implies greater load sharing between bone and implant in the deep and flush models versus in the protruding model. The major reason that the protruding model showed greater stress shielding than the deep and flush models is implant positioning. Such stress may also be due to the relatively high loading conditions, likely to be related to higher positions. A metal implant is stiffer than the surrounding soft-tissues, such as cartilage. Most loading was exerted on the implant due to the implant position in the protruding model, which led to less stress on the femoral cartilage and bone, resulting in stress shielding.

In terms of clinical relevance, our results showed the importance of the implant position in focal knee defect surgery. This has implications for surgical practice, with precision being highly dependent on the individual surgeon's technique and experience. In fact, most surgeons try to operate so that the joint line is maintained during surgery. However, our computational studies showed that preserving the joint line yields negative results in terms of contact stress of cartilage.

In addition, the lowest contact stress on the tibial cartilage in the deep model does not imply that deep surgery is required, because the deep model increases

loading in the lateral tibial cartilage due to force equilibrium.

This study had three limitations. First, the computational model was developed using data from a single, normal subject. Abnormal tibiofemoral alignment and distribution of weightbearing between the medial and lateral compartments of the tibia, which leads to a medial lesion, were not included in the model. However, the advantage of a computational simulation of a single, normal subject is the ability to determine the effects of material properties within the same subject, and exclude the effects of variables such as weight, height, bony geometry, ligament properties, and component size.<sup>10</sup> Second, the articular cartilage was considered as an elastic material, and the effects of anisotropy and viscoelasticity were not considered. The instantaneous response of cartilage to a short-term gait load was evaluated in this study; therefore, cartilage can be modelled as an elastic material.<sup>16</sup> Third, the simulations were only performed under static load because the ideal dynamic joint motion was too prohibitive in terms of computational and time efficiency. In future studies, dynamic FE simulations examining imbalance loading between medial and lateral sides should be performed for complete gait-cycle loading and boundary conditions, to better predict the biomechanics of the knee joint, with a possible extension to also study the biomechanical effects of focal knee arthroplasty size.

In conclusion, our results suggest that resurfacing with a focal knee arthroplasty does not threaten immediate deleterious effects on the opposite surfaces based on the contact pressure, as evaluated through the computational simulation of the deep model. Our results showed that significant surgical imprecision and protruding implants can lead to severe cartilage damage and delay bone union. Further investigation of metallic implants is required, due to the need for the utmost precision when it comes to positioning. Moreover, the long-term in vivo effects must be evaluated.

## References

1. Hangody L, Feczko P, Bartha L, Bodó G, Kish G. Mosaicplasty for the treatment of articular defects of the knee and ankle. *Clin Orthop Relat Res*. 2001;391 Suppl:S328–36.
2. Duan M, Wang Q, Liu Y, Xie J. The role of TGF- $\beta$ 2 in cartilage development and diseases. *Bone Joint Res*. 2021;10(8):474–487.
3. Custers RJH, Dhert WJA, van Rijen MHP, Verbout AJ, Creemers LB, Saris DBF. Articular damage caused by metal plugs in a rabbit model for treatment of localized cartilage defects. *Osteoarthritis Cartilage*. 2007;15(8):937–945.
4. Becher C, Huber R, Thermann H, et al. Effects of a surface matching articular resurfacing device on tibiofemoral contact pressure: results from continuous dynamic flexion-extension cycles. *Arch Orthop Trauma Surg*. 2011;131(3):413–419.
5. Koh JL, Wirsing K, Lautenschlager E, Zhang LO. The effect of graft height mismatch on contact pressure following osteochondral grafting: a biomechanical study. *Am J Sports Med*. 2004;32(2):317–320.
6. Bingham JT, Papannagari R, Van de Velde SK, et al. In vivo cartilage contact deformation in the healthy human tibiofemoral joint. *Rheumatology (Oxford)*. 2008;47(11):1622–1627.
7. Ryd L. The mini-metal concept for treating focal Chondral lesions and its possible application in athletes. *Aspetar Sports Medicine Journal*. 292–295. <https://www.aspetar.com/journal/viewarticle.aspx?id=309> (date last accessed 27 June 2023).
8. Kang K-T, Koh Y-G, Son J, et al. Finite element analysis of the biomechanical effects of 3 posterolateral corner reconstruction techniques for the knee joint. *Arthroscopy*. 2017;33(8):1537–1550.
9. Kang KT, Koh YG, Son J, Kwon OR, Park KK. Flexed femoral component improves kinematics and biomechanical effect in posterior stabilized total knee arthroplasty. *Knee Surg Sports Traumatol Arthrosc*. 2019;27(4):1174–1181.
10. Kang KT, Koh YG, Son J, Kwon OR, Lee JS, Kwon SK. Influence of increased posterior tibial slope in total knee arthroplasty on knee joint biomechanics: A computational simulation study. *J Arthroplasty*. 2018;33(2):572–579.
11. Koh YG, Son J, Kwon SK, Kim HJ, Kang KT. Biomechanical evaluation of opening-wedge high tibial osteotomy with composite materials using finite-element analysis. *Knee*. 2018;25(6):977–987.
12. Périé D, Hobatho MC. In vivo determination of contact areas and pressure of the femorotibial joint using non-linear finite element analysis. *Clin Biomech (Bristol, Avon)*. 1998;13(6):394–402.
13. Kayabasi O, Ekici B. The effects of static, dynamic and fatigue behavior on three-dimensional shape optimization of hip prosthesis by finite element method. *Materials & Design*. 2007;28(8):2269–2277.
14. Haut Donahue TL, Hull ML, Rashid MM, Jacobs CR. How the stiffness of meniscal attachments and meniscal material properties affect tibio-femoral contact pressure computed using a validated finite element model of the human knee joint. *J Biomech*. 2003;36(1):19–34.
15. Yao J, Funkenbusch PD, Snibbe J, Maloney M, Lerner AL. Sensitivities of medial meniscal motion and deformation to material properties of articular cartilage, meniscus and meniscal attachments using design of experiments methods. *J Biomech Eng*. 2006;128(3):399–408.
16. Peña E, Calvo B, Martinez MA, Palanca D, Doblaré M. Why lateral meniscectomy is more dangerous than medial meniscectomy. A finite element study. *J Orthop Res*. 2006;24(5):1001–1010.
17. Kim YS, Kang K-T, Son J, et al. Graft extrusion related to the position of allograft in lateral meniscal allograft transplantation: biomechanical comparison between parapatellar and transpatellar approaches using finite element analysis. *Arthroscopy*. 2015;31(12):2380–2391.
18. Kang K-T, Kim S-H, Son J, Lee YH, Kim S, Chun H-J. Probabilistic evaluation of the material properties of the in vivo subject-specific articular surface using a computational model. *J Biomed Mater Res B Appl Biomater*. 2017;105(6):1390–1400.
19. Koh Y-G, Lee J-A, Kim PS, Kim H-J, Kang K, Kang K-T. Effects of the material properties of a focal knee articular prosthetic on the human knee joint using computational simulation. *Knee*. 2020;27(5):1484–1491.
20. Brown TD, Pope DF, Hale JE, Buckwalter JA, Brand RA. Effects of osteochondral defect size on cartilage contact stress. *J Orthop Res*. 1991;9(4):559–567.
21. Guettler JH, Demetropoulos CK, Yang KH, Jurist KA. Osteochondral defects in the human knee: influence of defect size on cartilage rim stress and load redistribution to surrounding cartilage. *Am J Sports Med*. 2004;32(6):1451–1458.
22. Guettler JH, Demetropoulos CK, Yang KH, Jurist KA. Osteochondral defects in the human knee: influence of defect size on cartilage rim stress and load redistribution to surrounding cartilage. *Am J Sports Med*. 2004;32(6):1451–1458.
23. Brown TD, Pope DF, Hale JE, Buckwalter JA, Brand RA. Effects of osteochondral defect size on cartilage contact stress. *J Orthop Res*. 1991;9(4):559–567.
24. Huber-Betzer H, Brown TD, Mattheck C. Some effects of global joint morphology on local stress aberrations near imprecisely reduced intra-articular fractures. *J Biomech*. 1990;23(8):811–822.
25. Convery FR, Akeson WH, Keown GH. The repair of large osteochondral defects. An experimental study in horses. *Clin Orthop Relat Res*. 1972;82:253–262.
26. Stålmán A, Sköldenberg O, Martinez-Carranza N, Roberts D, Högström M, Ryd L. No implant migration and good subjective outcome of a novel customized femoral resurfacing metal implant for focal chondral lesions. *Knee Surg Sports Traumatol Arthrosc*. 2018;26(7):2196–2204.
27. Saris DBF, Dhert WJA, Verbout AJ. Joint homeostasis. The discrepancy between old and fresh defects in cartilage repair. *J Bone Joint Surg Br*. 2003;85-B(7):1067–1076.
28. Kirker-Head CA, Van Sickle DC, Ek SW, McCool JC. Safety of, and biological and functional response to, a novel metallic implant for the management of focal full-thickness cartilage defects: Preliminary assessment in an animal model out to 1 year. *J Orthop Res*. 2006;24(5):1095–1108.
29. Martinez-Carranza N, Berg HE, Hulthén K, Nurmi-Sandh H, Ryd L, Lagerstedt AS. Focal knee resurfacing and effects of surgical precision on opposing cartilage. A pilot study on 12 sheep. *Osteoarthritis Cartilage*. 2013;21(5):739–745.

### Author information:

- J-A. Lee, MS, Researcher
- K-T. Kang, PhD, Research Director, Professor  
Department of Mechanical Engineering, Yonsei University, Seoul, South Korea.
- Y-G. Koh, MD, Orthopedic Surgeon, Department of Orthopaedic Surgery, Yonsei Sarang Hospital, Seoul, South Korea.
- P. S. Kim, MD, Orthopedic Surgeon, Department of Orthopaedic Surgery, The Bone Hospital, Seoul, South Korea.
- J-H. Park, MD, Surgeon, Department of Anesthesiology & Pain Medicine, Hallym University College of Medicine and Kangdong Sacred Heart Hospital, Seoul, South Korea.

### Author contributions:

- J. Lee: Writing – review & editing.
- Y. Koh: Writing – original draft.
- P. S. Kim: Data curation.
- J-H. Park: Supervision.
- K-T. Kang: Supervision.

■ J-A. Lee and Y-G. Koh contributed equally to this work.

■ J-H. Park and K-T. Kang contributed equally to this work.

### Funding statement:

- The authors received no financial or material support for the research, authorship, and/or publication of this article.

### Data sharing:

- All data generated or analyzed during this study are included in the published article and/or in the supplementary material.

### Open access funding:

- The authors confirm that the open access fee for this article was self-funded.

© 2023 Author(s) et al. This is an open-access article distributed under the terms of the Creative Commons Attribution Non-Commercial No Derivatives (CC BY-NC-ND 4.0) licence, which permits the copying and redistribution of the work only, and provided the original author and source are credited. See <https://creativecommons.org/licenses/by-nc-nd/4.0/>